

On the Model Tests and Design Method of Hybrid CRP Podded Propulsion System of a Feeder Container Ship

Noriyuki Sasaki¹, Mariko Kuroda¹, Junichi Fujisawa¹,
Takanori Imoto², Masaharu Sato³

¹National Maritime Research Institute (NMRI), Tokyo, Japan

²Imoto Lines, Kobe, Japan

³Yanmar Co., Ltd., Tokyo, Japan

ABSTRACT

The application of podded propulsion technology has developed significantly in the last decade. The fitting of podded drives to conventional vessels such as cruise ships is now considered routine with new developments such as the double acting tanker (DAT) further advancing the pod concept. One of the more recent successful applications has been the hybrid contra-rotating podded propulsion outfitted on high-speed RO/RO vessels. However despite these advances there is little published data on the testing procedures and analysis of hybrid CRP podded propulsion systems for full-scale ships due to their complexity.

The hybrid CRP podded drive system is attractive to designers as it uses the energy saving advantages of the contra-rotating propeller effect. However, the system may also be susceptible to adverse off design conditions such as steering during course keeping whilst under normal navigation conditions. In this context, the design of hybrid CRP systems should be an optimal synthesis of several conflicting conditions such as propulsion, course keeping and berthing. In this paper, a design method for hybrid CRP podded drive systems together with analysis procedure of the subsequent model test results will be discussed.

Keywords

Hybrid CRP Podded Propulsion, Trade Off Design, Sea Margin

1 OBJECTIVE OF THE PROJECT

The ethos behind the research presented in this paper was a common design task, simply the replacement of 2 ageing container vessels with a single more efficient design of equivalent capacity. To achieve this goal numerous design scenarios were theorised, resulting in 3 essential parameters identified for the new design.

- Select maximum ship length, which will be allowed by port limitation.

- Adopt a hybrid CRP podded drive system.
- Evaluate transportation efficiency by taking account of the wave and wind effect of actual sea states.

1.1 Principal Dimensions

To satisfy the principal dimensions for the new design a review was conducted including a logistical simulation of an inland container service. From this study the optimum dimensions of the new vessel were carefully investigated and 3 candidate designs were proposed; these are given in Table 1.

Table 1 Principal dimensions for the proposed vessels

	Case 1	Case 2	Case 3	Case 4
<i>L_{PP}</i> (m)	87	110		
<i>Breadth</i> (m)	14	18.8		
<i>Depth</i> (m)	6.9	9.2		
<i>draft</i> (m)	3.65	6		
<i>DWT</i> (ton)	1810	4620		
<i>Design Speed</i> (kts)	14	17	17	14
<i>Propulsion System</i>	Single Screw	Single Screw	Hybrid CRP Podded propulsion System	

In addition to the powering requirements for calm seas condition, a further study was conducted for the added resistance increase in regular waves using the empirical formulae shown below.

$$Raw = C_1 \times \frac{1}{2} \rho g (1 + C_2 Fn_B^{0.8}) \times \zeta_a^2 \times B \times Bfcp \dots (1)$$

where,

$$Fn_B = Vs / \sqrt{gB} \dots \dots \dots (2)$$

$$Bfcp = \frac{1}{1 + [2 \times (1 - Cpf) \times Lpp / B]^2} \dots (3)$$

$$\left. \begin{aligned} C_1 &= 1 \\ C_2 &= 2 + 110 \times (0.3 - Bfcp) \quad \text{for } Bfcp \leq 0.3 \\ C_2 &= 2 \quad \text{for } Bfcp \geq 0.3 \end{aligned} \right\} \dots(4)$$

Where, R_{aw} is resistance increase in regular waves. V_s is ship speed in m/sec, ζ_a is amplitude of significant wave height in m, L_{pp} and B is ship length (m) and breadth (m) respectively, C_{pf} is prismatic coefficient of fore body. Coefficients C_1 and C_2 are derived from a data base obtained from sea keeping tests of typical existing ship models such as tankers, bulk carriers, container ships and car carriers.

If the resistance increase in regular waves can be represented as the above mentioned formula, resistance in short crested irregular waves can be obtained by a following simple equation.

$$\overline{R_{aw}} = \frac{1}{2} R_{aw} \quad \dots\dots\dots(5)$$

Results of calculations based on the above equations are shown in Figure 1. Beaufort Scales are given in Table 2.

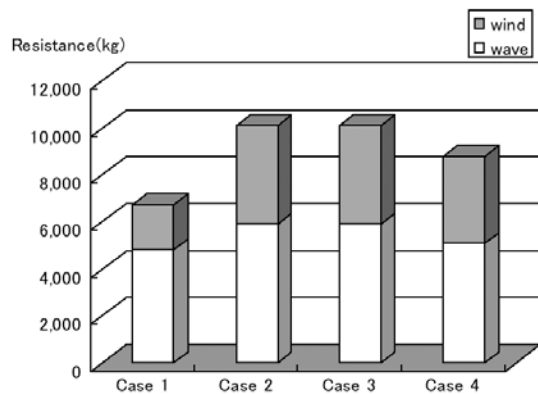


Figure 1 Added Resistance due to Wave and Wind at BF5

Table 2 Beaufort Scale

Beaufort scale	Mean wind velocity	Significant wave height	Mean wave frequency
5	9.8m/s	2 m	5.5 sec.
6	12.6 m/s	3 m	6.7 sec.

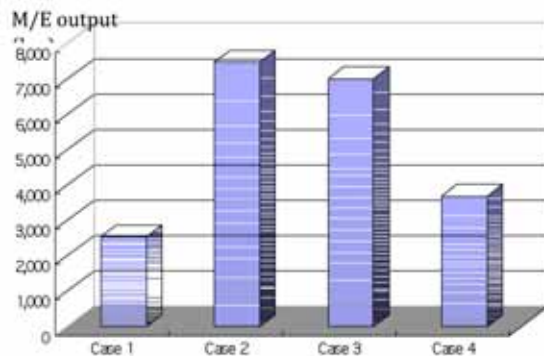


Figure.2 Predicted Engine Output (kw)

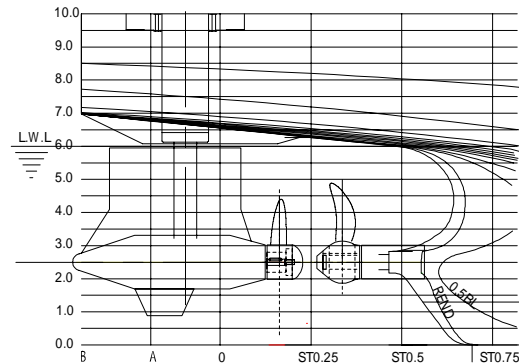
According to the calculated added resistance due to wave and wind, power losses are calculated taking propeller efficiency at highly loaded conditions into account. The results are presented in Figure 2 whilst the required main engine output including sea margins are shown in Table 3.

Table.3 Calculated Sea Margins and M/E Output

Ship	Case 1	Case 2	Case 3	Case 4
Sea Margin	64%	34%	33%	50%
MCR (kW)	2542	7494	7011	3687

1.2 Hybrid CRP Podded Propulsion System

From the analysis of 3 different ship types, the hybrid CRP podded propulsion system was selected as the preferred option as the system shows the best economical index ($DW \cdot V_s / BHP$). The forward propeller was directly driven by a conventional diesel engine and the aft propeller was driven by electric podded system which also negated the need for the use of a rudder. The power balance between the 2 propulsors was set at 60-66% to avoid operating the aft propeller outside of the forward propeller's slipstream. This propulsion concept was important, not only for cavitation but also for propulsive efficiency. The



schematic drawing of the hybrid CRP podded propulsion system is shown in Figure 3.

Figure 3 Schematic Drawing of Hybrid CRP Podded Propulsion System.

2 CRP DESIGN

2.1 NMRI CRP Design Program

Propellers of CRP system were designed based on CRP design program developed at NMRI; the program can be summarised as follows:

- Database of self propulsion factors for conventional single screw ships can be used.
- Power balance of two propellers can be easily changed.
- Different rpm for each propeller can be used

- Different wake fraction for each propeller can be used

The flow diagram of CRP design is shown in Figure 4.

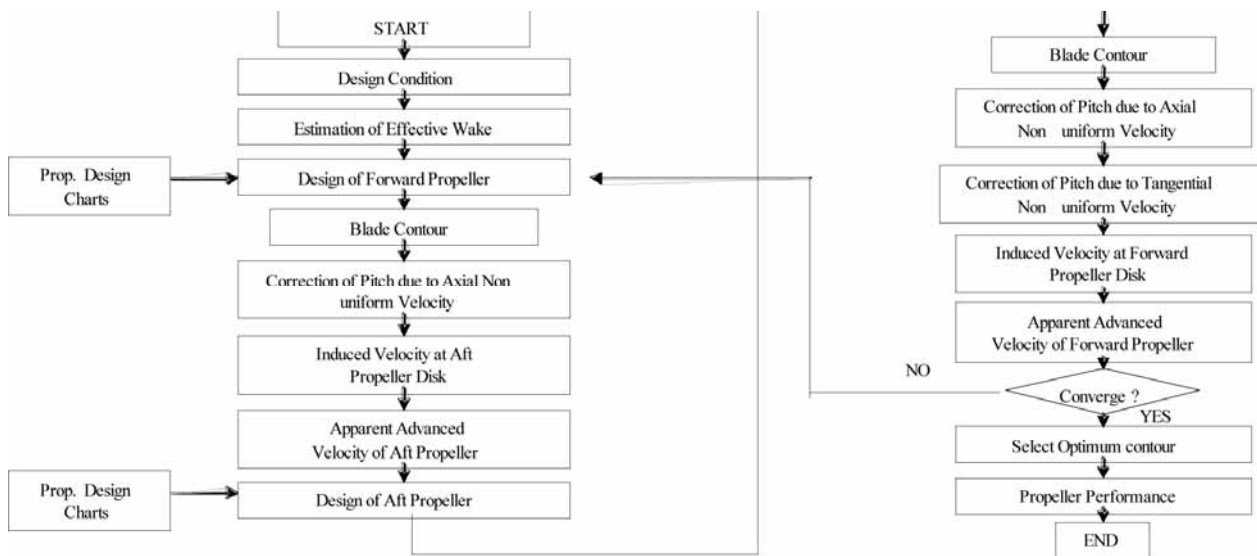


Figure.4 CRP Design Flow Diagram

2.2 OFF DESIGN CONDITION

As mentioned previously, during normal operation a podded propulsion system may be exposed to high levels of cavitation and vibration together with remarkable power loss due to the abrupt change in the propulsive efficiency of the pod propulsor. Therefore, the optimum design of the propulsor will be affected by the course keeping ability of a podded vessel. If the vessel has a poor course keeping capability, the designer should change the propeller design from the optimum open water condition; Figure 5 highlights this issue.

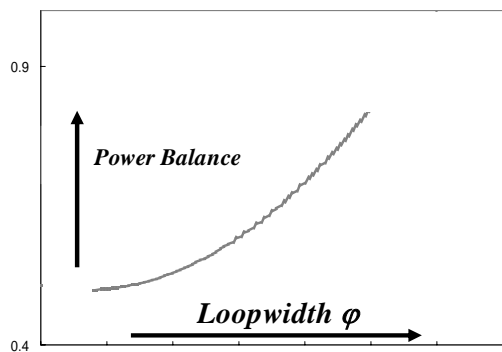


Figure 5. Power Balance of Hybrid CRP Pod Design.

Figure 5 indicates that a ship with a poor course keeping ability should allocate larger power to the forward propeller to avoid excessive disturbance by the aft propeller during the steering mode when the function of rudder is required from the podded propulsor.

Figure 6 shows the typical power tendency of CRP pod propellers during steering conditions. In the case of behind condition (ship wake), tangential component of ship wake induces unbalanced power between port and starboard side. In contrast, a symmetrical power increase can

be expected for the uniform wake case including a propeller operating in open water condition.

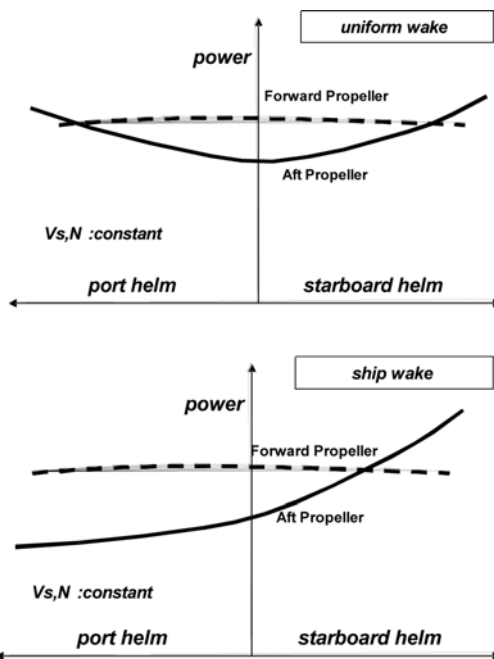


Figure 6 Typical power tendency of CRP Pod Propellers

3 MODEL TEST

There is very little information in the open literature describing the best procedure for performing model test with a hybrid CRP podded propulsion system. It seems that small number of facilities are conducting these tests with lack of confidence in their findings owing to the complex nature of the tests. The most serious issue associated with the test is the availability of full scale data for verification and validation of the results. Under these similar circumstances model tests of a hybrid CRP podded propulsion system were conducted at Mitaka No.2 ship experiment tank which has dimensions of 400m x

18m x 8m) at NMRI, Japan. A CRP propeller model and ship model were used in the experiments, they were manufactured to a scale of 1:19.092. Using this system 3 types of tests were performed to evaluate the performance of a designed vessel during navigation. The tests included propeller open water tests, self-propulsion test and resistance tests. The scope of the model tests is shown in Figure 7 and detail of each model test is explained in the following sections.

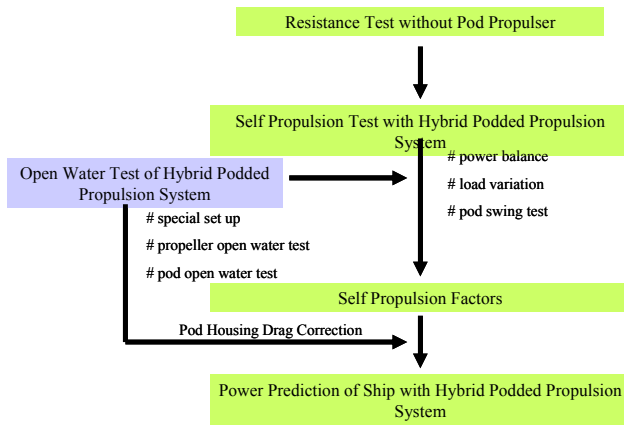


Figure 7 Required Model Tests for Hybrid Podded Propulsion System

3.1 Hybrid CRP Pod Open Water Test

For the Azimuthing Podded Propulsion the International Towing Tank Conference (ITTC) recommended procedure were developed and established by the 24th and 25th Special Committees. These Committees considered the podded propulsion system as one propulsion unit analogous to a conventional propeller. However, hybrid CRP podded system are significantly more complex when compared to a conventional podded propulsion system as the forward propeller should be driven by a propeller boat located in front of the forward propeller as shown in Figure 8. Therefore, in the case of Hybrid CRP pod open water testing, the most difficult problem during testing will be the presence of the propeller open boat required to drive the forward propeller. There is no favourable solution at the moment to eliminate the undesirable interference effects between a POT boat and the forward propeller. The effects are mainly associated with the wake from the shadowing effect of the POT boat and free surface effect generation by the POT boat, mostly from the strut of main boat. Under these circumstances the following types of tests should be recommended as a standard Hybrid CRP pod open water test.

1. Conventional propeller open water test of a forward propeller and an aft propeller
2. Propeller open water test of a forward propeller behind a POT boat (back to front)
3. Configuration 2 with a dummy pod
4. Pod open water test according to ITTC 2008 procedure
5. Hybrid CRP pod open water test

The purpose of each set up is explained in the Table 4 and some of those set up are shown in Figure 9.

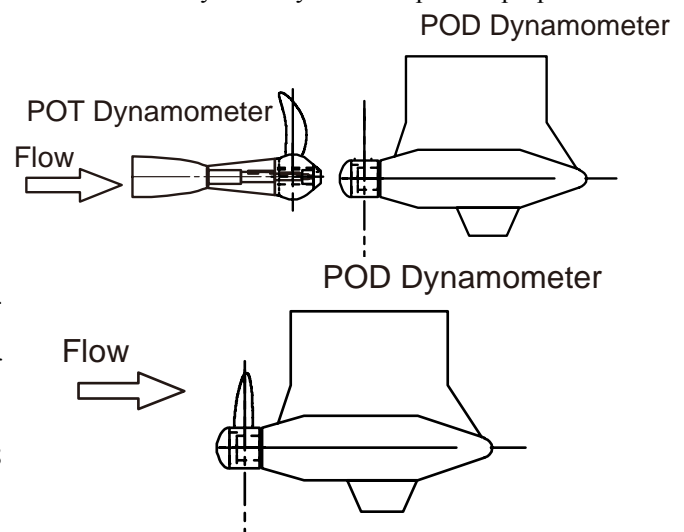


Figure 8 Arrangement of Hybrid CRP

Table.4 Purpose of Each Test

Test	Set Up	purpose of each set up (FP; forward propeller, AP; aft propeller, POC; propeller open water characteristics)
1	Conventional propeller open water test of a forward propeller	Obtain POC of FP and AP which will be used ConFigure.2/3//5 and ConFigure.4 respectively
2	Propeller open water test of a forward propeller behind a POT	Obtain wake fraction of open boat
3	ConFigure.2 with a dummy pod	Obtain potential wake fraction of dummy pod Eliminate negative pressure on a boss end of FP
4	Pod open water test according to ITTC 2008 procedure	Obtain POC of podded propulsion system
5	Hybrid CRP pod open water test	Obtain POC of Hybrid CRP open water characteristics

Figure 9 Additional model tests of hybrid pod POT. The research indicated that it was advantageous to describe and analyse the hybrid CRP podded propulsion



system as a unit propulsor analogous to the podded propulsion system. This treatment allows testing facilities to capitalise on all of their valuable resources, garnered from conventional model tests such as conventional propulsion systems with single screw propellers.

Using the above procedure a Hybrid CRP POT was conducted. Table 5 shows the particulars of model propellers. Test condition is shown in Table 6.

Table 5 Particulars of model propellers

Particular	forward	aft
D_{PF} [m]	0.2500	0.1990
x_B	0.267	0.274
H/D_{PF}	0.830	1.063
a_E	0.460	0.440
Z	4	5

For the study a series of propeller revolutions, which gave the same thrust balance (identity!) as self propulsion test were investigated. The thrust balance can influence the propulsion factors during an experiment (thrust deduction factor and wake fraction) by the interactions between the propeller, rudder and hull. According to this procedure, it was confirmed that sharing rate of the thrust force was 6:4, the same as that of the self-propulsion test shown in Figure 9. It is clear therefore that when performing open water tests it is important not to conduct the test at the designed propeller revolutions for both propellers to analyse the propulsive efficiency. It is also important to conduct the self propulsion test with the design power (or thrust) balance (do you mean identity?) to obtain the correct propulsion factors.

Table 6 Test condition of Hybrid CRP POD Open Water Test

Immersin	[%Dpf]	150%
n_{pF}	[rps]	8.95
n_{pA}	[rps]	10.00

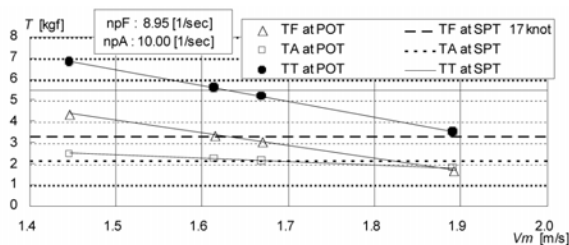


Figure.10 Sharing Rate of the Thrust Force at Open Water Test

3.2 Analysis of Hybrid Pod Open Water Test

Figure.11 shows mean velocities obtained by a forward propeller based on the thrust identity and nominal wake

measured by a Pitot rake. Both results show good agreement.

As mentioned previously, a hybrid CRP open water test cannot avoid the effect of non-uniform flow that originates from the open boat system of the forward propeller. The propeller boss cap is likely to suffer from measurable negative pressure, therefore placement of a long dummy boss from pod housing ahead of the forward propeller will help eliminate this effect.

In addition it may be possible to use the torque identity instead of thrust identity.

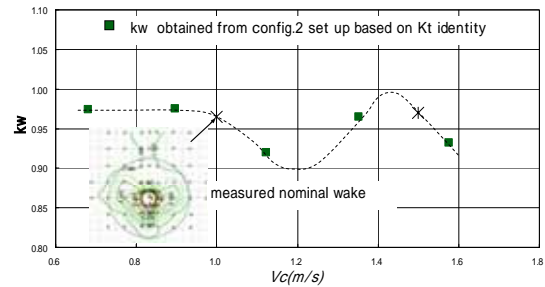


Figure.11 Mean Velocity at a Forward Propeller Plane behind Propeller Open Boat

Using one of these methods, propeller open water efficiency of a hybrid Pod CRP system can be represented as follows:

$$\left. \begin{aligned} \eta_o &= \frac{T_F \times V_{AF} + T_{UNIT} \times V_{AA}}{2 \times \pi \times (n_F \times Q_F + n_A \times Q_A)} \\ K_{TT} &= \frac{T_F + T_{UNIT}}{\rho \times n_F^2 \times D_F^4} \\ K_{QT} &= \frac{n_F \times Q_F + n_A \times Q_A}{\rho \times n_F^3 \times D_F^5} \end{aligned} \right\} (6)$$

Where, T_F is thrust of forward propeller and T_{UNIT} is thrust of Pod unit. Q_F and Q_A is torque of forward propeller and aft propeller, respectively; n_F and n_A is revolutions of forward and aft propellers, respectively; V_{AF} and V_{AA} is advanced speed of forward and aft propeller, respectively.

If the difference of advanced velocity of two propellers is negligibly small, then,

$$\eta_o = \frac{(T_F + T_{UNIT}) \times V_A}{2 \times \pi \times (n_F \times Q_F + n_A \times Q_A)} \dots \dots \dots (7)$$

Here, V_A is the mean velocity obtained from the above explained method and is shown in Figure 11. The result of open water efficiency of the hybrid system compared with a conventional propeller is shown in Figure 12.

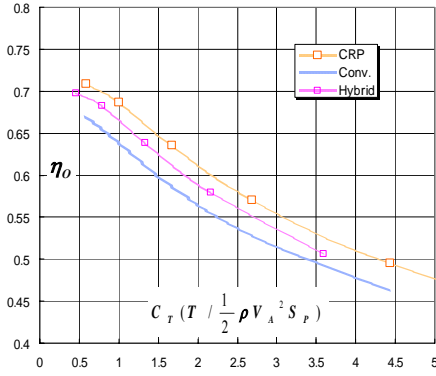


Figure 12 Open Water Efficiency of Hybrid Pod

In Figure 12, C_T is propeller loading coefficient and S_p is propeller disc area. Then, open water efficiency of each system can be represented as follows;

$$\text{Hybrid: } \eta_o = \frac{(T_F + T_{UNIT} + \Delta T_{UNIT}) \times V_A}{2 \times \pi \times (n_F \times Q_F + n_A \times Q_A)} \quad \dots(8)$$

$$\text{CRP : } \eta_o = \frac{(T_F + T_A) \times V_A}{2 \times \pi \times (n_F \times Q_F + n_A \times Q_A)} \quad \dots(9)$$

Where, ΔT_{unit} is pod housing drag correction based on the ITTC procedure (ITTC 2005).

The open water efficiency of Hybrid Pod is less than CRP system, which was obtained from extracting propeller thrust of podded system instead of unit thrust. The difference of efficiency between the hybrid pod and conventional propeller is about 4 %, while with the CRP system is 7%. The efficiency loss of hybrid system compared with the CRP system originated from the pod housing drag effect, even when corrected to full scale based on the ITTC standard method.

3.3 Resistance and Self Propulsion Test

ITTC (2008) procedures specified a dedicated testing procedure for a model test using a podded propulsion system. According to this procedure, the resistance test should be performed without the pod unit installed. This means that the pod housing effect will be included in propulsor part of the procedure as the interaction between pod and propeller is too significant compared with interaction between conventional rudder and propeller. It is generally recognized however, that the scale effect of the pod housing cannot be accounted for in the same manner as a conventional rudder, which has been included as a part of the hull wetted surface area. Therefore, there are no special issues involving resistance test for the hybrid CRP.

Propulsion test for the Hybrid CRP was conducted using the ship model with principal particulars shown in Table 8. Model tests were conducted in Mitaka No 2 ship experiment tank; the results of the self propulsion tests are shown in Figure 12. Also given is the self propulsion

factors of the single propeller (forward propeller of the hybrid CRP).

Table 8 Principal Dimensions of Model Ship

	Ship	Model
L_{PP} [m]	110.00	5.7616
L_{wl} [m]	117.32	6.1450
Breadth [m]	18.80	0.9847
Depth [m]	9.20	0.4714
draft[m]	6.00	0.3143

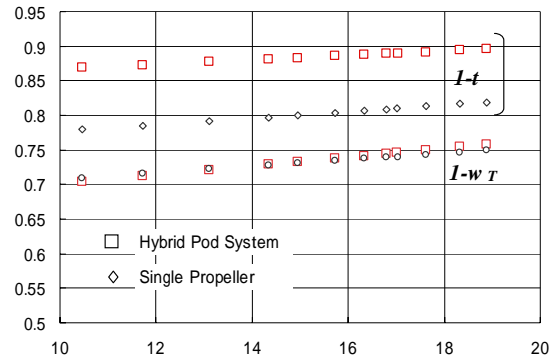


Figure.13 Comparison of Self Propulsion Factors between Hybrid CRP and the Single propeller

As shown in Figure 13, the wake fraction of the hybrid system is almost the same as that of the single conventional propeller if the whole hybrid system including pod housing is treated as a single propulsor system. The difference of thrust deduction comes from the existence of a rudder for single propeller's case. As the hybrid pod system has no rudder system the interaction between propeller and the hull is all that should be taken into account.

One of the key aspects which has been widely overlooked during these tests is the effect of power (or thrust) balance at the self propulsion conditions. In order to obtain the correct interaction between 2 propellers, hull and a rudder the power (or thrust) balance is the most dominant factor. The measurements should therefore be conducted at the target power balance conditions during self propulsion tests.

4 POWER CALCULATION

Power calculation was conducted according to ITTC (2008) recommended procedure. Delivered power curves are shown in Figure 14. From this figure it was established that the difference between single propeller and hybrid pod at the design speed 17kts was about 10%.

Another important aspect of the design was the economical evaluation; 2 vessels and 2 design conditions were investigated. Table 9 shows the principal dimensions and design speeds of the 2 vessels. Figure 15 to-

gether with the bottom row of Table 9 shows the results of the comparison based on a transportation efficiency ($DW*Vs/BHP$) taking transmission losses of electric drive into account. Here transmission losses of the hybrid system and conventional single propeller are calculated as follows;

$$\eta_i (\text{conventional}) = 0.96$$

$$\eta_i (\text{hybrid}) = 0.96 \times 0.6 + 0.86 \times 0.4 = 0.92$$

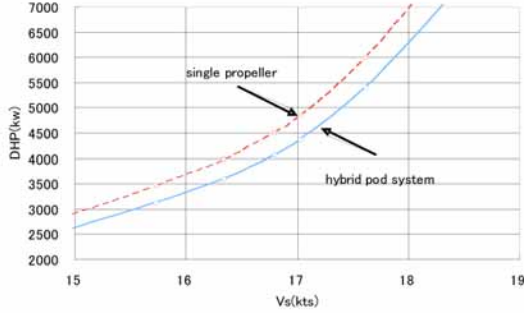


Figure 14 Comparison of Power (DHP) Curves

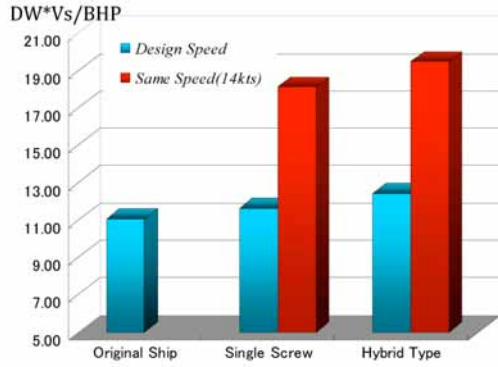


Figure 15 Economical evaluation of candidate designs

As shown in Figure 15 and Table 9, the Hybrid solution shows the best transportation efficiency among the 3 vessels investigated. The ratio of hybrid to the original design at the same speed is almost a 2 fold increase.

Table 9 Economical Evaluation of Present Ship

	original	single	hybrid	hybrid
L_{PP} (m)	87.0	110.0		
Breadth (m)	14.0	18.8		
Depth (m)	6.9	9.20		
draft(m)	3.65	6.00		
DW (ton)	1810	4620		
Design Speed(kts)	14.0	17.0	17.0	14.0
$DW*Vs/BHP$ (kw)	11.1	11.6	12.4	19.5

5 CHECKING ON THE OFF DESIGN CONDITION

As mentioned in Section 2.2, the correct power balance is a critical design parameter and so the final design should

be confirmed by model tests and computations. For example, simulation of manoeuvring motions in rough seas is an effective method to evaluate the hybrid pod propulsion system in an off design condition as the pod helm angles are necessary to maintain course.

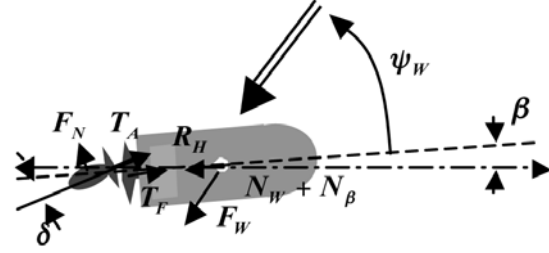


Figure 16 Hydrodynamic forces acting on a ship with hybrid pod propulsion

For equilibrium of motion, following equations are introduced;

$$\begin{aligned} X : R_H \cos \beta + F_W \cos \psi_w - T_F + T_A \cos \delta + F_N \sin \delta &= 0 \\ Y : R_H \sin \beta - F_W \sin \psi_w + T_A \sin \delta + F_N \cos \delta &= 0 \quad \dots(10) \\ N : N_W + N_\beta - T_A \sin \delta L_{SP} - F_N \cos \delta \times L_{AP} &= 0 \end{aligned}$$

Where,

N_β is yaw moment of the ship and R_H is ship resistance of approaching direction. F_W, N_W are wind and added wave resistance and moments due to rough sea and L_{AP} is a distance between centre of gravity and AP position. L_{SP} is a distance between COG and propeller position.

By solving equations, minimum δ can be obtained. In order to predict precise hydrodynamic forces, for the system a PMM (Planar Motion Test) or oblique going test.

Another aspect relevant to the evaluation of the hybrid design was the cavitation and efficiency of pod at the manoeuvring motion. It was obvious that the harmful cavitation occurred on the blade tip when the blade of pod propeller was exposed to the outside slipstream from the forward propeller, this could be avoided by adopting a smaller diameter podded propeller. However, risk of the hub vortex from the forward propeller impinging on the surface of pod propeller still remains an issue. A solution to this problem may be the use of a cylindrical hub or other counter measure to weaken the vortex strength.

The propulsive efficiency of hybrid pod system at the condition given in Figure 16 can be represented as below;

$$\eta_D = \frac{(T_F + T_{UNIT} \times \cos \delta + \Delta T_{UNIT}) \times (1-t) \times V_A}{2 \times \pi \times (n_F \times Q_F + n_A \times Q_A)} \quad \dots(11)$$

Figure 17 shows the result of calculations based on equation(11). The main reason of non-symmetrical shape for a propulsive efficiency at small helm angle is difference of pod housing drag. The housing drag at starboard side helm shows the higher resistance than port side helm. Therefore, pod unit thrust will decrease remarkably with starboard side helm.

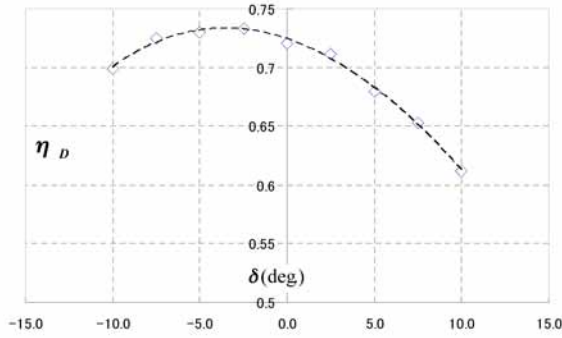


Figure 17 Propulsive Efficiency at Small Helm Angle of Hybrid Pod System

6 CONCLUSIONS

The hybrid CRP pod propulsion system is an extremely complex propulsion system, the advantages and disadvantages of this technology are not fully understood just yet. In this paper a procedure of model tests for hybrid pod system was presented and discussed. Through the theoretical study and findings from the model test the following conclusions are made:

1. Design methodology of hybrid pod system was proposed and verified by model testing.
2. Hybrid pod system can be a good solution for reduction of CO₂ emission because the system shows the best index for transportation efficiency amongst those studied.
3. Further investigation for non-symmetrical tendency of hybrid pod system for small helm angle is needed to avoid a poor navigation operation.
4. Power balance of hybrid pod system is the most important and it should be varied depending on a course keeping ability of the design ship.

7 REFERENCES

Atlar M., Woodward M., Besnier, F., Rosendahl T., Konieczny L., Ayaz Z. & Depascale R. (2006) "FAST-POD Project: An over all summary and conclusions" 2nd International Conference on Technical Advances in Podded Propulsion (T-Pod), Nantes, France.

Allenstrom B. & Rosendahl T. (2006), "Experience from testing of pod units in SSPA's large cavitation tunnel." 2nd International Conference on Technical Advances in Podded Propulsion (T-Pod), Nantes, France.

25th ITTC Specialist Committee on Azimuthing Podded Propulsion (2008), "Report of 25th ITTC Specialist Committee on Azimuthing Podded Propulsion" Proc. of 25th ITTC, Vol.2, Fukuoka, Japan

Sasaki N., Laapino J., Fagerstrom, B., Juurmaa, K. & Wilkman, G. (2004) "Full Scale Performance of Double Acting Tankers *Tempera & Mastera*", 1st International Conference on Technical Advances in Podded Propulsion (T-Pod), Newcastle upon Tyne, UK.

Appendix 1

Transformation from Regular Waves to Irregular:

An average value of resistance increase in irregular waves can be represented by a following equation using ISSC wave spectrum $S_{\zeta}(\omega)$;

$$\overline{R_{AW}} = 2 \int_0^{\infty} \frac{R_{AW}(\omega)}{\zeta a^2} \cdot S_{\zeta}(\omega) d\omega \dots (A1)$$

Here, assuming modified Pierson-Moskowitz type ,

$$\left. \begin{aligned} S_{\zeta}(\omega) &= \frac{K_1}{\omega^5} e^{-\frac{K_2}{\omega^4}} \\ K_1 &= 0.11 H_{1/3}^2 \omega_T^4 \\ K_2 &= 0.44 \omega_T^4 \end{aligned} \right\} (A2)$$

Where, $\omega_T = 2\pi / T_0$ T_0 is mean wave period.

If the resistance increase of regular waves can be represented by

$$R_{AW} = C_1 \times \frac{1}{2} \rho g (1 + C_2 F_{nB}^{0.8}) \times \zeta a^2 \times B \times B f_{cp} \dots (A3)$$

By substituting equation (A2) and (A3) to equation(A1),

$$\overline{R_{AW}} = 2 \cdot C_1 \cdot 1/2 \cdot \rho g (1 + C_2 F_{nB}^{0.8}) \cdot B \cdot B f_{cp} \cdot \int_0^{\infty} S_{\zeta}(\omega) d\omega \dots (A4)$$

An integral part can be reduced analytically as follows;

Then,

$$\begin{aligned} \int_0^{\infty} S_{\zeta}(\omega) d\omega &= \int_0^{\infty} \frac{K_1}{\omega^5} e^{-\frac{K_2}{\omega^4}} d\omega \\ &= \frac{1}{2} \times R_{AW} \dots (A6) \end{aligned}$$